INTEGRATION OF VARIOUS ENERGY SOURCES PV/FUEL CELL AND BATTERY-OPERATED MULTI-LEVEL INVERTER FOR AC LOAD

Ch. Anil Kumar, UG Student, Sree Vahini Institute of Science and Technology (Autonomous), Tiruvuru, Andhra Pradesh
D. Lakshmi, UG Student, Sree Vahini Institute of Science and Technology (Autonomous), Tiruvuru, Andhra Pradesh
Y. Bharath Gopi, UG Student, Sree Vahini Institute of Science and Technology (Autonomous), Tiruvuru, Andhra Pradesh
U. Ashok, UG Student, Sree Vahini Institute of Science and Technology (Autonomous), Tiruvuru, Andhra Pradesh
Mrs. Hari Priya Asst. Professor, Dept of EEE, Sree Vahini Institute of Science and Technology (Autonomous), Tiruvuru, Andhra Pradesh
Dr. K. Kiran Kumar Assoc. Professor, Dept of EEE, Sree Vahini Institute of Science and Technology (Autonomous), Tiruvuru, Andhra Pradesh

Abstract:
The system under consideration is constructed using Matlab/Simulink; the outcomes demonstrate the efficacy of the proposed technique and demonstrate that it is feasible with a research circumstance. The present study analyzes an electrical energy production system which consists of three energy sources: a battery, a fuel cell, and photovoltaic energy. For controlling every component, this hybrid manufacturing system is optimized. Additionally, a multilevel inverter in the hybrid system circuit lowers the harmonic rate by enhancing the quality of energy raised into the alternating load. For minimizing load variations, an energy control algorithm is developed to maximize power flow in the various fabrication system stages. Matlab/Simulink is used to model and simulate a prototype which can be implemented in an experimental test bench in order to evaluate the strategy.

Keywords:
MPPT tracking, three-level inverter, fuel cell, battery, photovoltaic (PV), hybrid system and fuzzy logic control (FLC).

I.Introduction

The last several decades suffer from experienced a rise in interest in renewable energy sources, and significant research is being done to create effective systems for converting all of these into electrical power. Reducing environmental harm, conserving energy, reducing exhaustible sources and enhancing safety are the main goals of these methods. Power can be sent to an isolated demand or straight to a utility grid using renewable energy technologies.Stand-alone systems are more widely used in remote locations that are distant from the electric grid. Applications for integrating energy storage systems (ESSs) include load shifting, grid stability, consistent power quality, grid operational assistance and seamless power injection to the grid. The research literature is presented a number of power smoothing techniques [2] and in order to preserve power and energy balance and enhance power quality, battery energy storage systems (BESS) are chosen as energy storage and integrated into fuel cells and photovoltaic systems.

The fuel cell energy conversion system FC/PV generators function as the main energy source in the research study proposed Energy Management of multi-sources Power System PV/Fuel Cell and Battery Based Three Level Inverter, which also includes a battery energy storage system (as short and medium, time storage devices) [1]. A three-phase, three-level Neutral Point Clamping (NPC) converter is used to connect the entire system to the load and they are all connected to a DC voltage connection. Since there is no requirement for synchronization to integrate the energy sources, the DC coupled structure allows for greater flexibility in the system as a whole and allows for the free selection of both the quantity and type of energy sources. The RMS value of the load voltage is confirmed by using fuzzy logic control (FLC) for the operation of the three-level inverter attached to the load.

ISSN: 2278-4632
Vol-15, Issue-04, No.02, April: 2025

II.Details of the proposed System

The primary components of the multi-source system under analysis coupled to an AC load are depicted in fig.1.

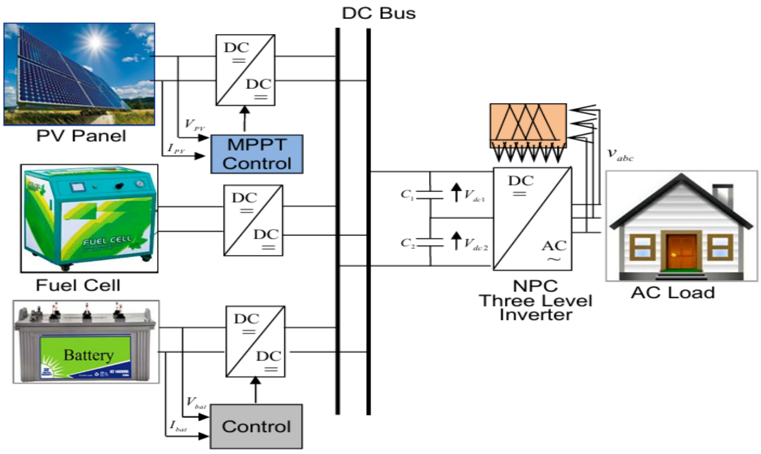

Fig.1. Diagram of the proposed multi-source PV/FC and battery system.

III.Solar PV modelling

PV cells are the most fundamental generating component of PV systems, which are based on solar energy. Figure 2 illustrates where a diode and a current source linked antiparallel with a series resistance constitute a photovoltaic cell [2].

In a single-diode cell, the relationship between voltage and current can be expressed as follows:

$$I_{PV} = I_{ph} - I_0 \left(\exp\left(\frac{q(V_{PV} + R_{s\,mod} I_{PV})}{AKT} \right) - 1 \right) \ \ldots \ (1)$$

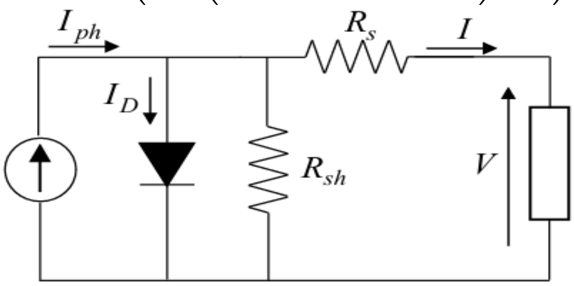

Fig. 2. PV cell equivalent circuit

Boost converter DC/DC and MPPT (Maximum Power Point Tracking)

A step-up DC/DC converter known as a boost converter raises the solar voltage to the output voltage which the load demands. The setup is depicted in figure 3 and includes a DC input voltage in V, load resistance R, diode D1, capacitor C for filtering, inductor L, switch S and switch S.

The boost inductor stores energy from the input voltage source while switch S is turned on, and the charged capacitor regulates the load current throughout the duration to ensure that it remains constant. The input voltage and the stored inductor voltage will emerge across the load when switch S is off, increasing the load voltage. thereby, the duty ratio D determines when switch S is ON or OFF, which in turn determines the load voltage.

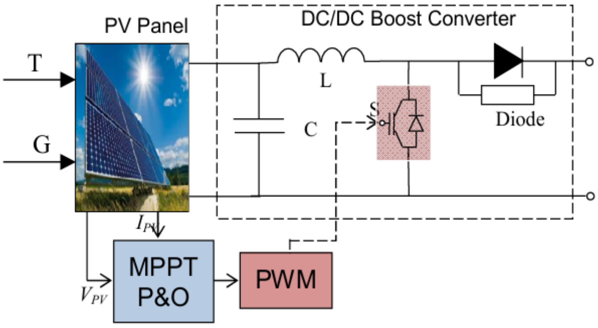

 ISSN: 2278-4632
Vol-15, Issue-04, No.02, April: 2025

Fig. 3. MPPT-controlled boost converter

The MPPT technology increases the efficiency of solar panels. The maximum power transfer theorem, which states that the load attains its maximum power when the source and load impedances are identical, is applied by the MPPT. In order to align the load impedance to the source, the MPPT modifies the duty ratio of the DC/DC converter and draws the most power possible from the solar cell.

Modeling of FC Systems

A dynamic model of the PEMFC is predicated on the correlation between the output voltage and the water, oxygen and hydrogen potential pressures. One can calculate the fuel cell stack total output voltage as follows: [3, 4].

$$V_{cell} = E_{nerst} - V_{act} - V_{ohmic} - V_{con} \quad \dots (2)$$

where E_{nernst} is the Nernst voltage, which is the thermodynamic voltage of the cells and is dependent on the temperatures and partial pressures of the reactants and products inside the stack; E_0 is the standard reversible cell potential (V); N_0 is the number of cells in the stack; R is the universal gas constant (8.3145 J·mol-1·K-1); T is the stack temperature (K); F is the Faraday's constant (96485 A·C·mol-1); and P_{H2}, P_{O2}, P_{H2O} are the partial pressures of hydrogen, oxygen, and water (atm), respectively.

$$\begin{cases} E_{nerst} = N_0 \left[E_0 \dfrac{RT}{2F} \log\left(\dfrac{P_{H2} P_{O2}^{0.5}}{P_{H2O}} \right) \right] \\ V_{ohmic} = R_m I \end{cases} \quad \dots (3)$$

Where K_{H2O}, K_{H2}, K_{O2} are the valve molar constants for water, hydrogen, and oxygen in (Kmol·s-1·atm-1), respectively.

$$\begin{cases} P_{O2} = \dfrac{1/K_{O2}}{1+\tau_{O2} s} \left(q_{O2}^{in} - 2K_r I \right) \\ P_{H2} = \dfrac{1/K_{H2}}{1+\tau_{H2} s} \left(q_{H2}^{in} - 2K_r I \right) \\ P_{H2O} = \dfrac{1/K_{H2O}}{1+\tau_{H2O} s} \left(2K_r I_{fc} \right) \\ q_{O2}^{in} = \dfrac{1}{1+T_f s} \left(\dfrac{2K_r}{U_{opt}} I_{fc} \right) \\ q_{O2}^{in} = \dfrac{1}{rHO} q_{H2}^{in} \end{cases} \quad \dots (4)$$

Where q_{O2}^{in}, q_{O2}^{in} and are the hydrogen and oxygen input flow (kMol/s), I is the stack current (A),$K_r = \frac{N}{4F}$ is the modeling constant, with N being the number of the series-wound fuel cells in the stack. $\tau_{H2}, \tau_{O2}, \tau_{H2O}$ are the time constants for hydrogen, oxygen and water in (sec), U_{opt} is the optimum fuel utilization, T_f is the fuel time constant (sec), rHO is ratio of hydrogen to oxygen [5, 6]. $V_{act}, V_{ohmic}, V_{con}$ are the activation, Ohmic and concentration polarizations losses respectively.

$$V_{act} = [\xi_1 + \xi_2 + \xi_{3T} \times \ln(C_{O2}) + \xi_4 T \times \ln(I)] \quad \dots (5)$$

Where ξ_i(i=1,2,3,4) are the parametric coefficients defined based on the kinetic, thermodynamic and electrochemical phenomena. C_{O2} is the concentration of oxygen dissolved in a water film interface in the catalytic of the cathode in (mol/m3). It is expressed as follows [5]

$$C_{O2} = \frac{P_{O2}}{5.08 \times 10^6 e^{-\frac{498}{T}}} \quad \dots (6)$$

The following represents the Ohmic polarization loss:

$$V_{ohmic} = IR_m \quad \dots (7)$$

The research derives ohmic resistance as R_m [6]. To express a concentration polarization, utilize:

$$V_{con} = -B \times \ln\left(1 - \frac{I}{I_{lim}}\right) \quad \dots (8)$$

ISSN: 2278-4632
Vol-15, Issue-04, No.02, April: 2025

With I_{lim} being the current density where fuel is used in a same rate as the maximum input rate (A/cm2). The quantity of electric energy collected from the FC should be estimated in order to size the fuel cell. The quantity of energy produced by the FC per kilogram of hydrogen needs to be estimated, which can be performed as follows [7]:

$$E_g^{FC} = H_2^{used} \xi_{fc} \frac{H_2\text{heating value}}{H_2\text{density}} \quad \text{... (9)}$$

Where H_2^{used} represents the quantity of hydrogen input to the FC in Kg, ξ_{fc} is the FC efficiency, H_2 heating value is equal to 3.4 kWh/m3 in the standard condition and H_2density is 0.09 Kg/m3.

IV.SYSTEM COMPONENT CONTROL

The control techniques that will be developed in this section are included in the multi-sources system depicted in Fig.1.

Modeling of Battery:

The battery is being modeled by a variety of editors, and based on studies conducted on lead/acid batteries, a model known as the "CIEMAT model" is developed to depict where the battery functions during the charge, discharge, and overcharge phases. A verified model for battery capacity is presented in our case study based on the conducted experiments for any size and type of lead/acid battery [8]. A voltage source, the open circuit voltage V, is connected in series with an internal resistance R in this diagram, which is represented by an analogous circuit model. The battery's output voltage is accordingly:

$$V_{bat} = V - RI_{bat} \quad \text{... (10)}$$

where changes in internal resistance, temperature and battery state of charge (SOC) affect both Vbat and Ibat.

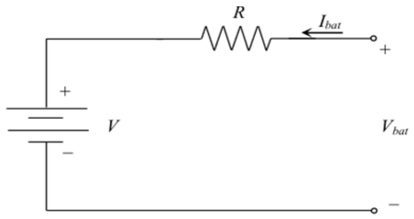

Fig. 4. The battery control

In the present study, the battery basic model, which is based on the CIEMAT model, is deemed accurate enough to evaluate power management objectives and compare the effectiveness of various approaches. [9] provides a description of the state of charge (SOC) in terms of time (t) during the charging and discharging operation.

$$SOC(t) = \begin{cases} SOC(t-\Delta t) + P_{bat} \dfrac{\eta_{ch}}{C_n V_{dc}} . \Delta t \\ SOC(t-\Delta t) + P_{bat} \dfrac{1}{\eta_{dis} . C_n . V_{dc}} . \Delta t \end{cases} \quad \text{... (11)}$$

where Δt is the time step, Pbat represents the battery power, Cn is the nominal capacity of the battery, ηch and ηdis are respectively the battery efficiencies during charging and discharging phase. Vdc denotes the nominal DC bus voltage. At any time step Δt, the SOC must comply with the following constraints.

$$SOC_{min} \le SOC(t) \le SOC_{max} \quad \text{... (12)}$$

The maximum and lowest permitted storage capacity are denoted by SOCmin and SOCmax, respectively.

Battery control

Controlling the battery current is the control system objective in order to achieve the necessary power. The model also incorporates maximum SOC constraints as well as charging and discharging current limits. As seen in figure 5, a bi-directional Buck-Boost DC/DC converter connects the BESS to the DC grid.

ISSN: 2278-4632
Vol-15, Issue-04, No.02, April: 2025

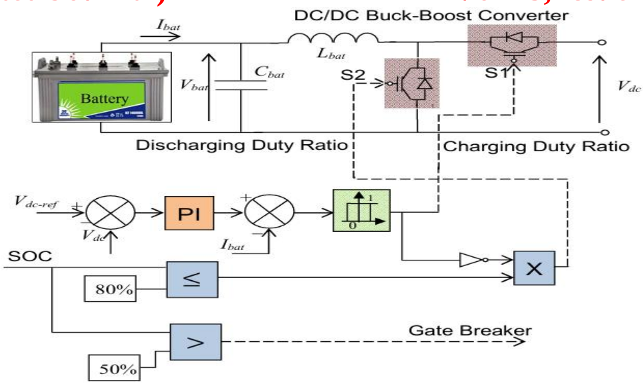

Fig.5. The battery control

Depending on the amount of energy needed, the BESS will function in charging, discharging, or floating modes. The DC bus voltage at the BESS point of connection controls these modes. As a result, the BESS must supply the requisite DC voltage level in various microgrid operating modes or AC load scenarios, like ours. When switch S2 is turned on, the converter functions as a boost circuit; when switch S1 is turned on, the converter functions as a buck circuit. Switch S1 is turned on when the DC link voltage is less than the voltage reference. On the other hand, switch S2 is triggered when the voltage at the DC connection exceeds the stated value. An intrinsic temporal constant characterizes the PV-battery system reaction to transient fluctuations. In these situations, the DC grid's capacitors can help fill the gap or absorb excess energy by acting as virtual inertia [10, 11, 12; 13, 14].

The design is possible to represent the DC-link power balancing using the differential equation which follows:

$$V_{dc}i_{dc} = P_{PV} + P_{FC} + P_{bat} - P_{load} \quad \dots (13)$$

The power balance of the integrated hybrid distributed generation system (DGS) with energy storage is controlled by the following factors, ignoring losses in the power converters, batteries, filtering inductors, transformer, and harmonics from switching actions:

$$V_{dc}i_{dc} = CV_{dc}\frac{dV_{dc}}{dc} = P_{PV} + P_{FC} + P_{bat} - P_{load} \dots \quad (14)$$

The capacitor voltage ripple is quite less than the steady-state value since the battery converter function is to sustain the voltage at the DC connection constant. Adjusting the capacitor voltage is the responsibility of the battery power if the powers injected by the two back-to-back voltage source converters (VSC) are considered to be constant at any particular time.

V.Simulation Results

The DC voltage of a three level (NPC) inverter linked to the multi-sources (PV-FC-battery) system integrated with an AC load is controlled by employing Fuzzy Logic Control (FLC) in the simulations conducted to verify the viability of the proposed strategy.

It is assessed under various load scenarios using MATLAB/Simulink software. In Tables 1, 2, 3 and 4, the suggested system parameters are mentioned. At time t= [0, 2, 3.5] s, the variable solar irradiation G = [600, 1000, 800] W/m2 and temperature T = 293 K determine the amount of electricity the PV array generates or supplies. Three different operating modes are available for the proposed system, contingent on the fluctuating load. Figs. 6 to 16 depict the system performance under these circumstances.

The active power, current, and voltage on the load with an FLC and a PI controller are displayed in figures 6, 14, and 15. It is evident that the burdens have increased. At [0, 3s], [3, 4s], [4, 5s], [5, 6s] and [6, 7s], respectively, a 7-kW, 14-kW, 7-kW, 10-kW and finally a 7-kW load were supplied to the system. Consequently, the system supplies a total load of 14 kW. The DC link voltage Vdc remains stable at the designated value (640V) with changing power, as shown in Figure 12. This is a significant benefit that demonstrates the efficacy of the proposed scheme. It is able to equalize the various input DC link voltages of the multilevel inverter by using it. The input voltages are then almost identical in pairs, as figure 12 depicts.

 ISSN: 2278-4632
Vol-15, Issue-04, No.02, April: 2025

The global (total) state of charge (SOCG) of storage devices is shown in figure 8. The system runs at full charge when the SOC is 60% between 0 and 2 seconds. As seen in figure 6, all of the storage devices are turned off since the combined power provided by the fuel cell and PV exceeds the load requirement.

The system enters the critical mode when the SOCG falls. For preserve the system equilibrium, the supervisory controller responds appropriately and cuts off the load with the lowest priority. All storage devices could be unplugged in the event of a power outage as it must request the utility of the deletion procedure. In addition, cannot approve the storage system charging method. These outcomes demonstrate the effectiveness of the controls and management applied to this hybrid system.

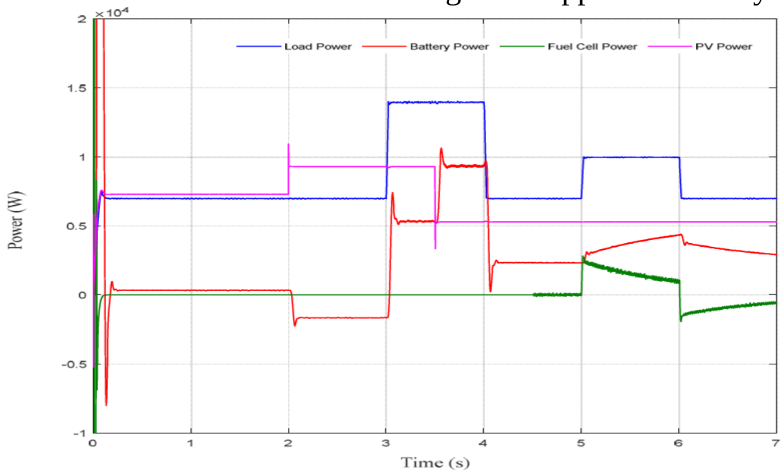

Fig. 6. The hybrid system power production under various AC loads

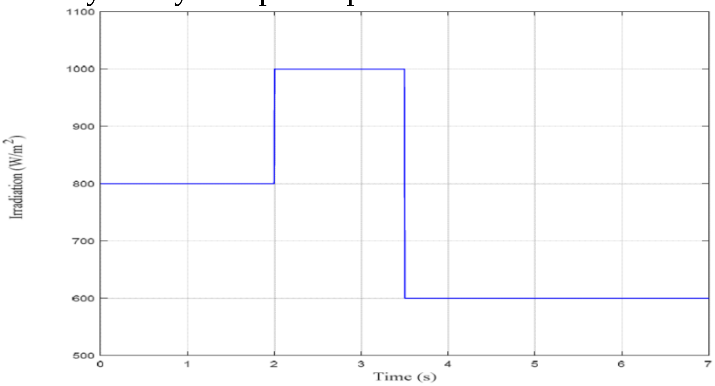

Fig.7. shows irradiation (W/m2).

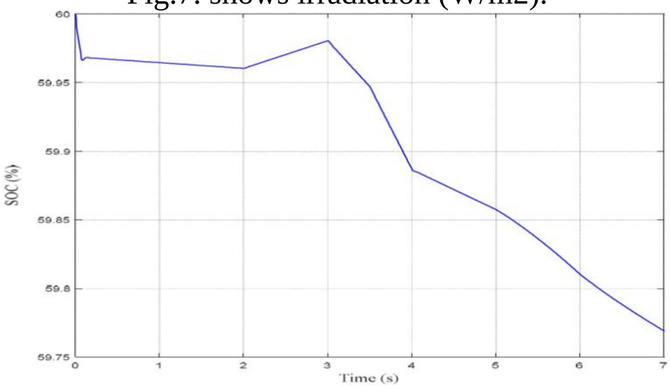

Fig. 8. Global state of charge of battery

ISSN: 2278-4632
Vol-15, Issue-04, No.02, April: 2025

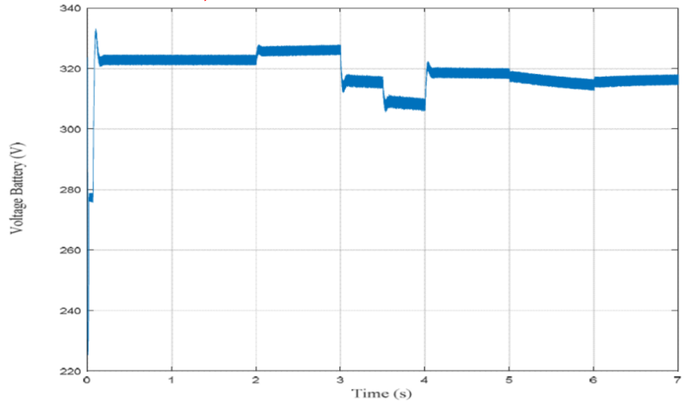

Fig.9. Battery Voltage

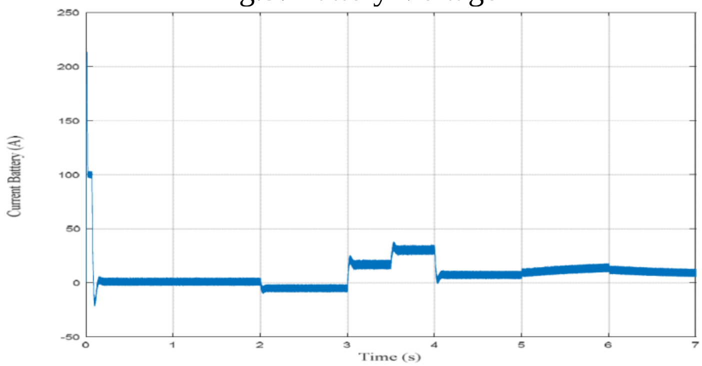

Fig.10. Battery Current

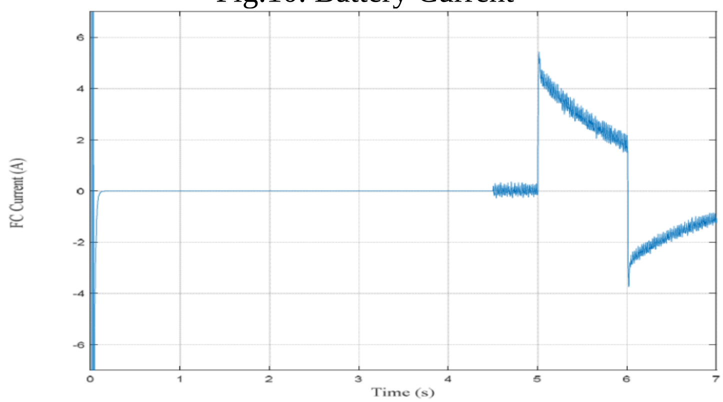

Fig. 11. Fuel Cell current

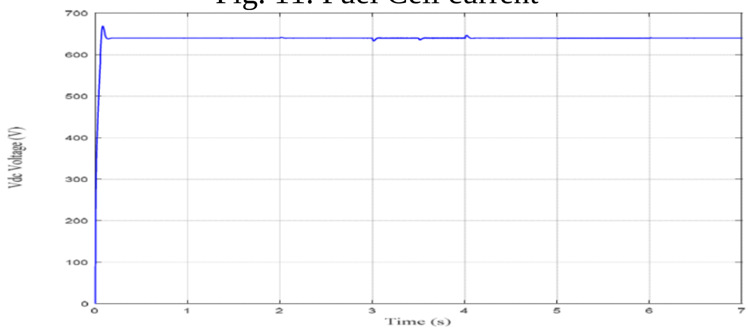

Fig. 12. DC link voltage

ISSN: 2278-4632
Vol-15, Issue-04, No.02, April: 2025

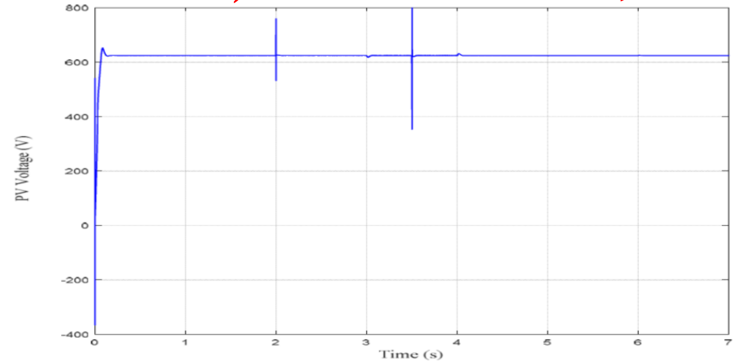

Fig. 13. Photovoltaic Model Output Voltage

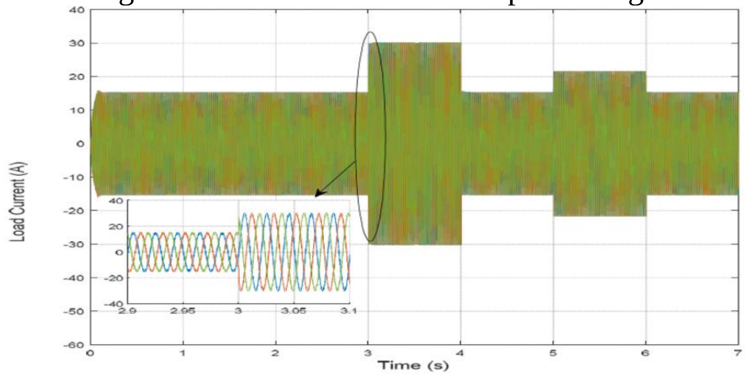

Fig. 14. AC load current

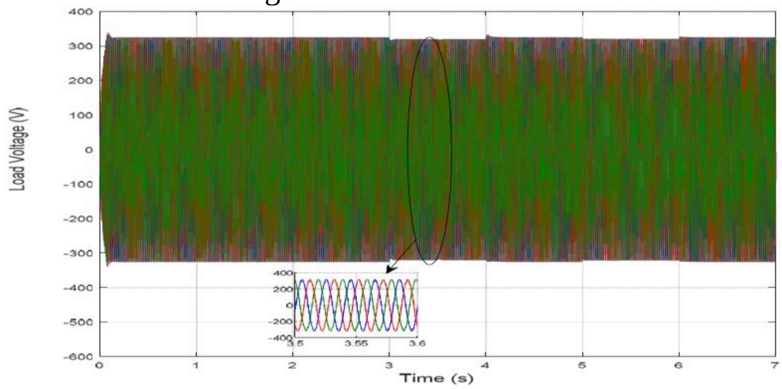

Fig. 15. AC load voltage

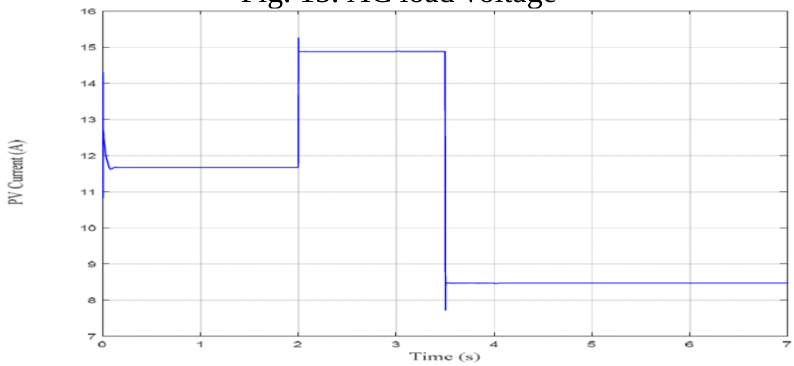

Fig. 16. Photovoltaic Model Output Current

VI.Conclusion

This paper presents a multi-source energy system that includes a battery and fuel cell/photovoltaic system. MATLAB/SIMULINK is suggested for dynamic modeling and simulations of the hybrid system. A hybrid energy system is being developed and tested, along with its supervisory battery voltage management. The PV array, FC and battery work together to meet load demand. The output from solar and FC systems is converted into AC power output using a three-level converter. An additional load can be connected and disconnected within the allotted period using a circuit breaker.

In order to fulfill the load, this multi-source system is managed to provide the greatest output power under all operating situations. The battery supports either a solar system or an FC to fulfill the load. Additionally, the battery supports the PV system and FC operating simultaneously under the same load.

These outcomes demonstrate the effectiveness of the controls and management employed for this hybrid system, which is widely implementable using the DSP or D space platform.

Table I: Parameters of Fuel Cells

Absolute temperature (K)	1273
Initial current (A)	50
Faraday's constant (C/kmol)	96.487e6
Universal gas constant J/(kmol K)	8314
Ideal standard potential (V)	1.18
Number of cells in series	450
Maximum, minimal and optimal fuel utilization	[8.43e-4 2.81e-4 2.52e-3]
Response time for hydrogen, water and oxygen flow (s)	[26.1 78.3 2.91]
Ohmic loss per cell (ohms)	3.2813e-004
Electrical response time (s)	2
Fuel processor response time (s)	5
Ratio of hydrogen to oxygen	0.145

Table II: Parameters of PV

Components	Rating values
Peak Power	200 W
Peak Voltage	660 V
Peak current	7.52 A
Open Circuit Voltage	33.2 V
Short Circuit Current	8.36 A

Table III: Parameters of Battery and AC Load

Components	Rating values
Load 1, 2, 3 (R)	7 kW, 7 kW, 3 kW
Battery type	Nickel Metal hydride
Nominal voltage	300 V
Capacity rating	6.5 AH

Table IV: Three Level NPC Inverter with DC/DC Bi-Converter

Components	Rating values
C_1=C_2	2.2 mF
Dc link Voltage	640 V
Frequency	50 Hz
Converter Inductor	5 mH
DC link Voltage	640 V
Converter Capacitor	2.2 mF

REFERENCES

[1] Nabil Karami, Nazih Moubayed, RachidOutbib, “Energy management for a PEMFC–PV hybrid system,” http://dx.doi.org/10.1016/ j. Encon man. 2014.02 070, Energy Conversion and Management 82 (2014) 154–168.

[2] V. Boscaino, R. Miceli, G. Capponi, G. Ricco Galluzzo, “A review of fuel cell-based hybrid power supply architectures and algorithms for household appliances,” 0360-3199/$ e see front matter Copyright ª 2013, Hydrogen Energy Publications, LLC. Published by Elsevier Ltd, http://dx.doi.org/10.1016/j.ijhydene.2013.10.165.

[3] Th. F. El-Shatter, M.N. Eskandar, M.T. El-Harry, “Hybrid PV/Fuel Cell System Design and Simulation,” 0960-1481/02/$ - see front matter 2002 Elsevier Science Ltd, PII: S09 60 - 1481(01)00062-3, Renewable Energy 27 (2002) 479–485.

[4] Phatiphat Thounthong, Arkham Luksanasakul, Podolska Kaseya porn, “Intelligent Model-Based Control of a Standalone Photovoltaic/Fuel Cell Power Plant with Supercapacitor Energy Storage,” IEEE Transactions on Sustainable Energy, VOL. 4, NO. 1, January 2013, 1949-3029/$31.00 © 2012 IEEE.

[5] Akbar Maleki, Alireza as Karameh, “Optimum Configuration of Fuel Cell-B PV/Wind Hybrid System using a Hybrid Metaheuristic Technique,” International Journal of Engineering & Applied Sciences (IJEAS) Vol.5, Issue 4 (2014)1-12.

[6] M. Calderon, A.J. Calderon, A. Ramiro, J.F. Gonzalez, “Automatic management of energy flows of a stand-alone renewable energy supply with hydrogen support,” International Journal of hydrogen energy 3 5 (2 0 1 0) 2 2 2 6 – 2 2 3 5. [7] Erkan Dursun, Osman Kilic, “Comparative evaluation of different power management strategies of a stand-alone PV/Wind/PEMFC hybrid power system,” 0142-0615/$ - see front matter _ 2011 Elsevier Ltd. doi: 10.1016/j.ijepes.2011.08. 025, “Electrical Power and Energy Systems 34 (2012) 81–89.

[8] A. Berkani, K. Negadi, T. Allaoui, F. Marignetti, “Fuzzy Direct Torque Control for Induction Motor Sensorless Drive Powered by Five Level Inverter with Reduction Rule Base,” Presland Elektro technic z, y, doi:10.15199/48.2019.07.14, No/Vol: 07/2019 Page no. 66.

[9] Juan P. Torreglosa, Pablo García-Triviño, LuisM. Fernández-Ramirez, Francisco Jurado, Control based on techno-economic optimization of renewable hybrid energy system frost and-alone applications,” http://dx.doi.org/10.1016/j.eswa.2015.12.038 0957-4174/© 2016 Elsevier Ltd, Expert SystemsWith Applications 51 (2016) 59–75.

[10] Koulali M. Mankour M., Negadi K., Mezouar A. (2019). Energy management of hybrid power system PV Wind and battery based three level converter, TECNICA ITALIANA-Italian Journal of Engineering Science, Vol. 63, No. 2-4, pp. 297-304. https://doi.org/10.18280/ti-ijes.632-426.

[11] Jingang Han, Jean-Frederic Charpentier and Tianhao Tang, “An Energy Management System of a Fuel Cell/Battery Hybrid Boat,” Energies 2014, 7, 2799-2820; doi:10.3390/en7052799.

[12] Omar Hazem Mohammed, Yassine Amirat, Mohamed Benbouzid, Adel Elbaset. Optimal Design of a PV/Fuel Cell Hybrid Power System for the City of Brest in France,” IEEE ICGE 2014, Mar 2014, Sfax, Tunisia.pp.119-123. hal-01023490.

[13] Pablo García, Juan P. Torreglosa, Luis M. Fernández, Francisco Jurado, “Improving long-term operation of power sources in off-grid hybrid systems based on renewable energy, hydrogen and battery,” Journal of Power Sources 265 (2014) 149e159

[14] A. Elbaset, “Design, Modeling and Control Strategy of PV/FC Hybrid Power System,” Journal of Electrical System 7.2 (2011): 270-286.

[15] Pablo Gracia, Juan P. Torreglosa, Luis M. Fernandez, Francisco Jurado, “Optimal energy management system for standalone wind turbine/photovoltaic/hydrogen/battery hybrid system with supervisory control based on fuzzy logic,” http://dx.doi.org/10.1016/j.ijhydene.2013.08.106, International Journal of Hydrogen Energy 38 (2013) 14146-14158.

[16] A. Berkani, K. Negadi, T. Allaoui, F. Marignetti, “Sliding mode control of wind energy conversion system using dual star synchronous machine and three level converters,” TECNICA ITALIANA-Italian Journal of Engineering Science, Vol. 63, No. 2-4, pp. 243-250. https://doi.org/10.18280/ti-ijes.632-418, 2019.

[17] Power management system for off-grid hydrogen production based on uncertainty,” International Journal of Hydrogen Energy 40 (2015) 7260 -7272